JOURNAL OF MATERIALS SCIENCE 15 (1980) 2573–2583

Mechanical properties of the Sn-Zn eutectic alloys

F. VNUK*, M. SAHOO†, D. BARAGAR‡, R. W. SMITH
Department of Metallurgical Engineering, Queen's University, Kingston, Canada

The structure and mechanical properties of Sn–Zn unidirectionally frozen eutectic alloys have been examined over the growth range 5 to 4000 mm h^{-1}. The structure is predominantly broken-lamellar below 750 mm h^{-1} but becomes increasingly fibrous at higher growth rates. The yield and ultimate strengths when tested in tension and compression were found to increase monotonically with growth rates up to 1000 mm h^{-1} above which they assumed near constant values. This behaviour is attributed to some loss of axial growth at higher growth rates. The hardness measured on transverse sections increased over the entire growth rate range. Annealing at near eutectic temperatures followed by quenching increased the strength of alloys grown at less than 750 mm h^{-1} and decreased that of those grown at higher rates. Similar behaviour was observed in selected Cd–Zn eutectic alloys. The increase in strength is attributed to solid solution hardening and the reduction to structural degradation during annealing. The Sn-rich matrix in this broken-lamellar eutectic appears to contribute significant strengthening to the composite.

1. Introduction

This study forms part of a general evaluation of eutectic alloys which has been in progress in the authors' laboratory for an extended period. Earlier work has been concerned principally with the development of a suitable morphological classification scheme [1–3] in order to be able to characterize eutectic structures sufficiently closely to permit a generalized description of mechanical and other properties.

It was found that the so-called anomalous eutectics were not in fact so, but could be placed in four well-defined categories, namely, broken-lamellar, irregular, complex-regular and quasi-regular, with increasing volume V_F of the faceting phase. With this classification scheme at hand, we have been examining systematically the extent to which the mechanical properties of each morphological group can be clearly characterized. To date we have reported work on Al–Si [4], Pb–Sb [5], Zn–Ge [6], Cd–Zn [7], Pb–Cd [8], Sb–Ge [9] and Cd–Ge [10].

This paper reports an investigation of the structure and mechanical properties of another simple binary eutectic system, Sn–Zn. On the basis of the eutectic classification suggested by Crocker *et al.* [1] this system has a eutectic structure of the broken-lamellar type, the volume fraction of faceting lamellar phase being 8.3%, the other being non-faceted. The tin-rich matrix has a body centred tetragonal structure ($a = 5.831$ Å, $c = 3.182$ Å) while the lamellae are composed of almost pure zinc, which has a close packed (c.p.) hexagonal structure ($a = 2.664$ Å, $c = 4.947$ Å). Thus it can be seen that the eutectic-forming components differ very distinctly in structure and lattice parameters, consequently, one might expect large variations in matrix constraints between the slowly-grown and fast-grown structures.

*Present address: School of Metallurgy, S.A. Institute of Technology, Adelaide, S.A., Australia.
†Present address: Canmet, Department of Energy, Mines and Resources, Ottawa, Canada.
‡Present address: Steel Company of Canada, Hamilton, Ontario.

0022–2461/80/102573–11 $03.10/0

2. Experimental procedures

Alloys of eutectic composition (91.4 wt.% Sn [11]) were prepared from "high purity" (i.e. 99.9995%) tin and zinc. Weighed amounts (in batches of 150 g) were sealed in argon-filled Pyrex tubes, melted in a gas flame and shaken to promote thorough mixing. After solidification by cooling in air, the samples were swaged to 4.7 mm diameter and cut into 22 cm lengths. These in turn were sealed in argon-filled Pyrex tubes of 5.1 mm internal diameter (i.d.) and directionally solidified by lowering through a tube furnace set at 450° C into a circulating water bath placed 1.5 cm below the furnace. Before lowering, the specimens were held for 30 min to establish equilibrium. It was found from preliminary measurements with 0.1 mm diameter wire thermocouples sealed transversely across the specimens that the growth velocity was equal to the lowering rate over most of the specimen length for the range of growth rates used ($1 \rightarrow 5000$ mm h^{-1}). The temperature gradient for an alloy grown at $R = 120$ mm h^{-1} was 80° C cm^{-1}.

After freezing, the specimens were removed from Pyrex tubes and 3 cm lengths from the top and the bottom were cropped-off and discarded. The remaining segment was cut into 3 compressive specimens (which were also used for transverse hardness testing) about 1.2 cm long; 2 specimens for microexamination (longitudinal and transverse) and one specimen about 7 to 8 cm long for tensile testing, the latter being done with a machined diameter of 3.8 mm and a gauge length of 5 cm.

The compression specimens were polished in special holders to produce parallel faces. Whilst in these they were tested for hardness (VPN), using a 1 kg load. The faces were then repolished to remove the hardness indentations.

Compressive and tensile testing were carried out on an Instron testing machine at a crosshead speed of 0.13 mm min^{-1}.

For metallographic investigation the specimens were mounted in a cold-setting resin, polished and then etched in dilute nitric acid.

In order to investigate the extent of the influence of the *in-situ* annealing occurring during the growth of the more slowly grown samples, selected specimens were immersed in an oil bath, maintained at 190 ± 2° C, for 5 min, water-quenched and then tested. For comparison Cd–Zn eutectic specimens were tested in the as-grown and heat-treated condition for a few selected growth rates.

3. Results

3.1. Microstructure

3.1.1. Morphology

The morphology of the Sn–Zn eutectic has been investigated previously by several groups of workers [12–14]. It has been generally agreed upon that the structure is "broken-lamellar" [12, 13], the Zn–lamellae being uneven in thickness and irregularly perforated. This perforation increases with increasing growth rate. The claim by Jaffrey and Chadwick [15] that the "fibres" of the Zn-phase always possess a ribbon-like morphology regardless of their growth rate could not be supported by the present investigation. In fact, as seen in Fig. 1, the usual broken-lamellar structure is produced at lower growth rates (up to approximately 1000 mm h^{-1}). This is demonstrated further in Figs. 2a, b, 3a, b and 4. The density and extent of perforation is highly growth-rate dependent. However, grains in which the Zn-phase tended to be ribbon-like were occassionally seen. At growth rates greater than approximately 1000 mm h^{-1} the broken-lamellar structure is so fine and so extensively fragmented by perforation as to have a fibrous appearance. This broken-lamellar → fibrous transition can be seen in Fig. 5 a to d.

3.1.2. Interlamellar Spacing

It has been established that the interlamellar spacing, λ, as measured on transverse sections of a lamellar eutectic and the solidification rate, R, should obey the relationship [16, 17]

$$\lambda^2 R = \text{const., or } \lambda = c/R^{-1/2} \qquad (1)$$

The variation of interlamellar spacing with growth rate for this system is shown in Fig. 6. It is seen that the slope of the plot of log λ versus log R yields a straight line but with a slope of only -0.42, rather than the value of -0.5 as predicted by Equation 1. However, the experimental value compares well with the figure of -0.44 reported by Tiller and Mrdjenovich [18].

3.2 Mechanical Properties

3.2.1. Tensile/compressive testing

The mechanical testing data are shown in Table I, Fig. 7 (tensile) and Fig. 8 (compressive). It is seen that the strength increases smoothly with the growth rate in this particular case up to $R \sim 1000$ mm h^{-1}. Beyond that value, the curves for yield and ultimate strength in both tension and compression tend to level-off.

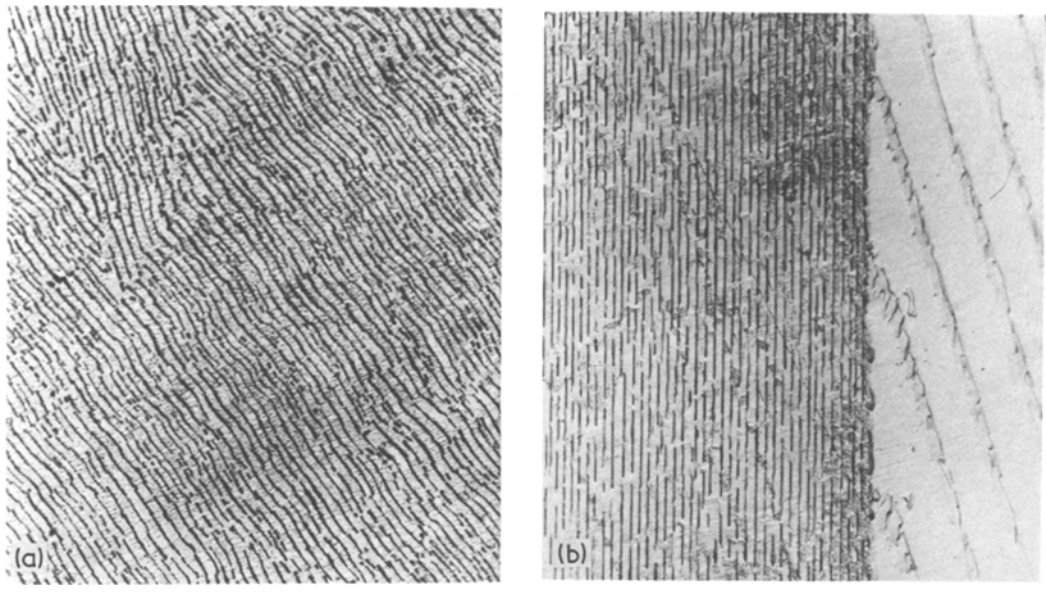

Figure 1 Optical micrographs of the directionally solidified Sn–Zn eutectic showing the broken-lamellar structure. Growth rate = 5 mmh^{-1}. a) transverse section (×480) b) longitudinal section (×480).

3.2.2. Hardness of Sn–Zn alloys

As with the tensile and compressive properties here too an increase in hardness occurs as the rate of solidification is increased, Fig. 9. Since the hardness values are more subject to local materials variations, considerable scatter was experienced, in spite of all the precautions taken in determining the hardness. The values in Table II represent averages of 12 to 20 readings on each specimen and show that the hardness of as-grown specimens rises smoothly with solidification rate.

3.2.3. Effect of heat treatment on mechanical properties

When dilute alloys of Zn in Sn are quenched from near-eutectic temperatures a marked increase in hardness occurs as compared with a slowly cooled sample [19]. It is known that Zn diffuses $\sim 10^3$

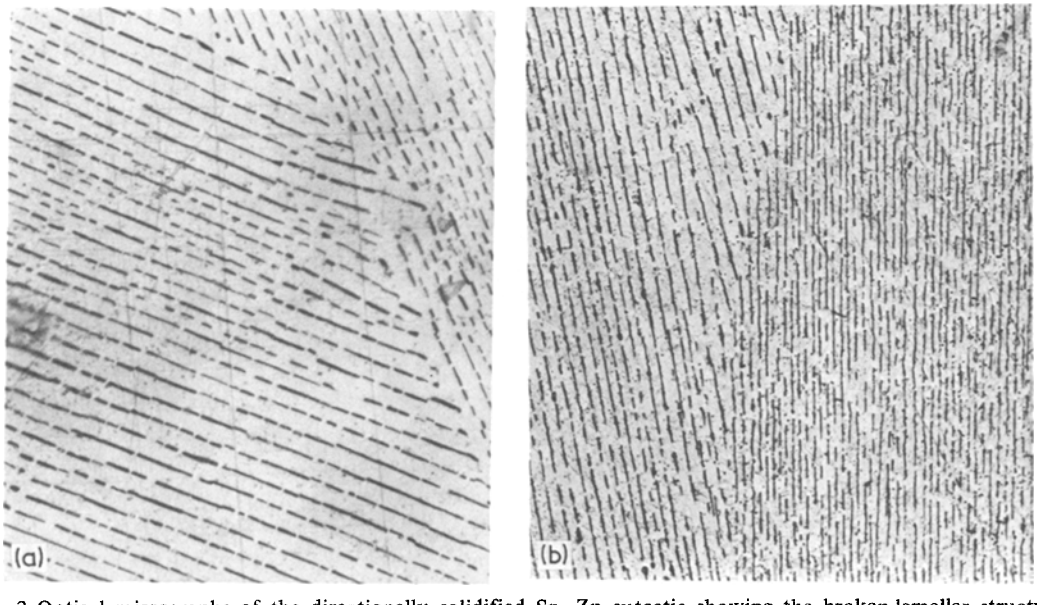

Figure 2 Optical micrographs of the directionally solidified Sn–Zn eutectic showing the broken-lamellar structure, growth rate = 12 mm h^{-1}. a) transverse section (×800) b) longitudinal section (×320).

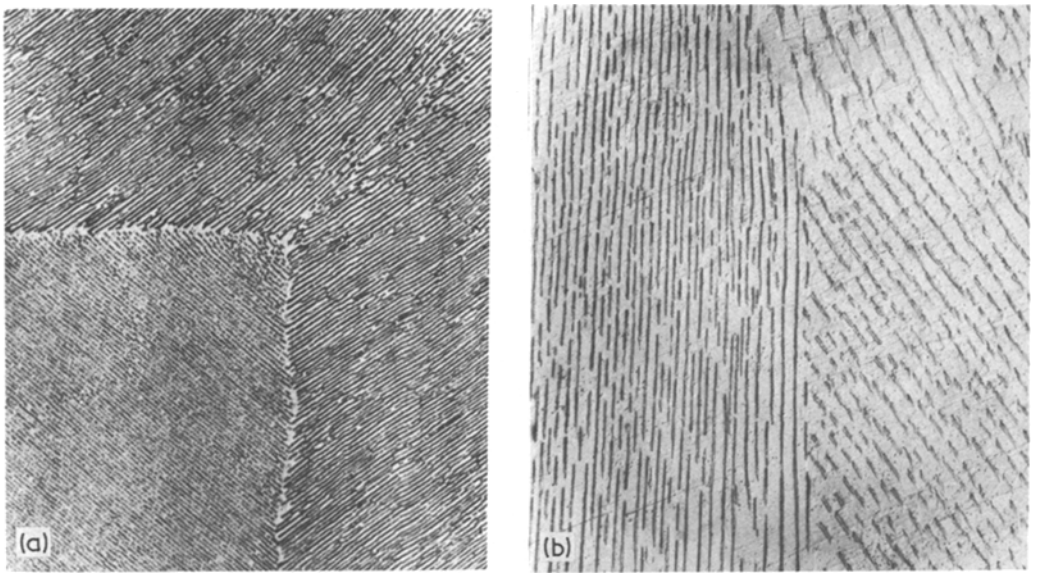

Figure 3 Optical micrograph of the directionally solidified Sn–Zn eutectic showing the broken-lamellar structure. Growth rate = 26 mm h^{-1}. a) transverse section (×480) b) longitudinal section (×480).

faster in the *c*-direction in tin than expected from a normal substitutional solute [20, 21] and so it is considered that the increase in hardness upon quenching arises because of the lattice strain associated with the trapping of fast-diffusing Zn ions in interstial positions between substitutional rest sites in the host Sn lattice [20]. In order to check whether this phenomenon contributed to the increased strength and hardness of the Sn–Zn eutectic alloys which were grown rapidly (and therefore cooled quickly), the effect of quenching eutectic specimens from 195° C on the strength and hardness was examined. The results are shown in Tables I and II and in Figs. 8 and 9. It is seen that there is an abrupt transition at approximately 750 mm h^{-1} from increased values for the mechanical properties of the more slowly-grown samples to decreased values for the more rapidly-grown specimens.

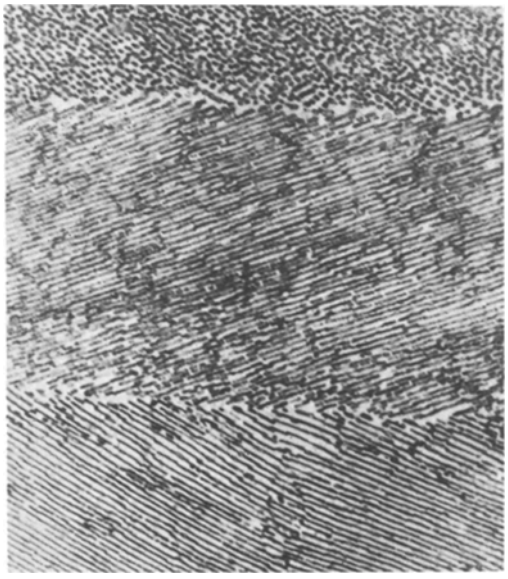

Figure 4 Optical micrograph of the directionally solidified Sn–Zn eutectic showing the broken-lamellar structure. Growth rate = 120 mm h^{-1}. Transverse section (×960).

Since these results were not quite as expected, it was decided to examine the effect of a "solutionizing" heat treatment, followed by quenching on the mechanical properties of eutectic specimens of Cd–Zn, a system not known to involve a fast-diffusing species. The results are shown in Table III, where a similar trend to that of Sn–Zn is noted.

4. Discussion

4.1. Microstructure

It is a common feature of non-faceted (N.F.)/faceted (F) eutectics that the faceting phase adopts a fibrous ("modified") morphology when rapidly frozen [1, 2, 3, 5]. However, unlike most of the systems examined, of which Al–Si [4] is typical, the Sn–Zn system does not appear to generate sufficient constitutional undercooling at large growth rates to cause dendrites of the non-faceting matrix phase (Sn) to appear. Even in the Cd–Ge eutectic with only 2 wt % of the faceting phase (Ge) present,

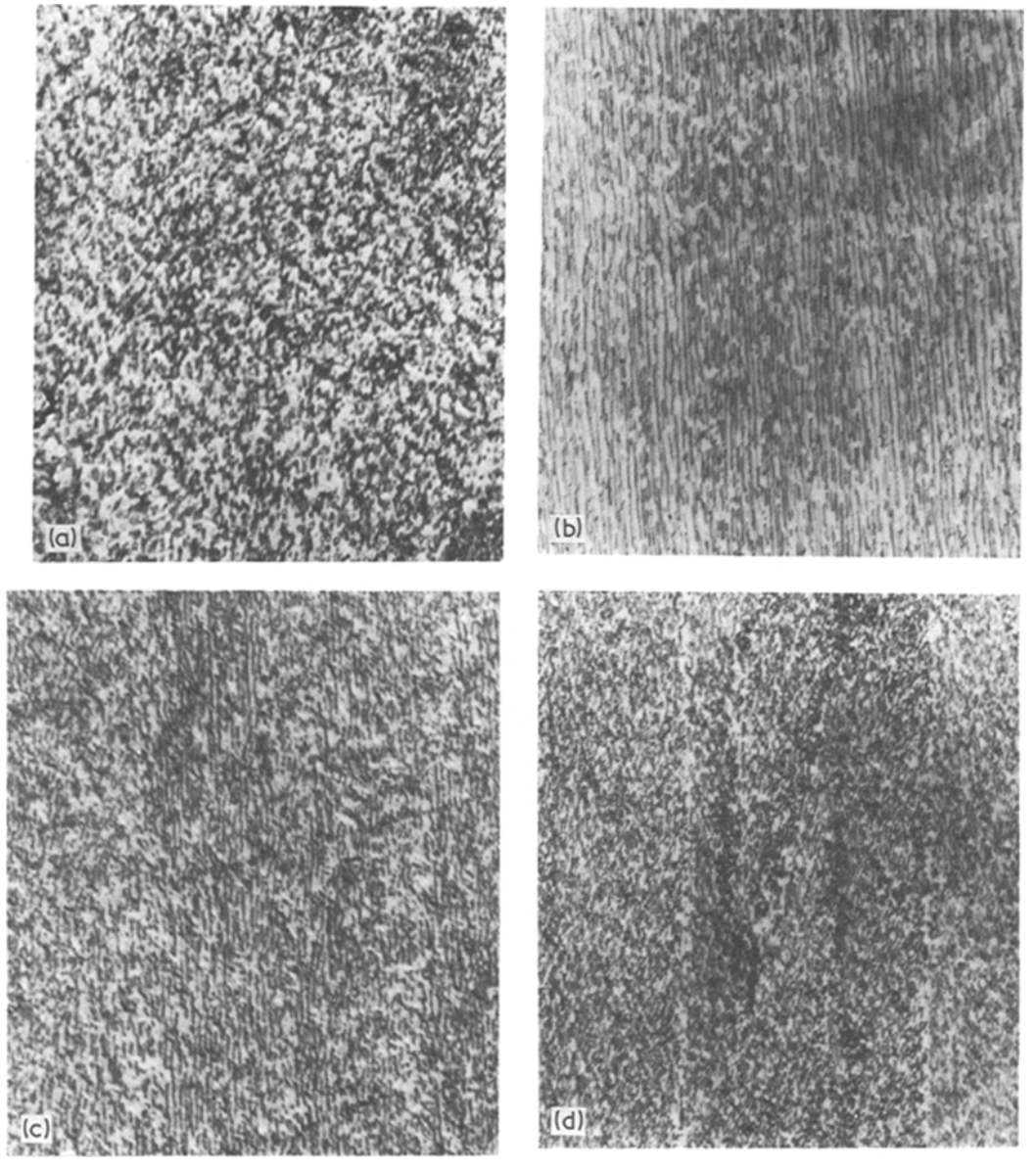

Figure 5 Optical micrographs of directionally solidified Sn–Zn eutectic showing the broken-lamellar → fibrous structural transition of the Zn-rich phase. (a) Growth rate 1200 mm h^{-1}. Transverse section (× 1200). (b) Growth rate 1200 mm h^{-1}. Longitudinal section (× 960). (c) Growth rate 2800 mm h^{-1}. Longitudinal section (× 960). (d) Growth rate 4000 mm h^{-1}. Longitudinal section (× 960).

Cd primaries appear readily for growth rates in excess of 100 mm h^{-1} when modest temperature gradients exist in the liquid.

In addition, it is noted that when $R \simeq$ 3000 mm h^{-1}, a growth rate well above that at which most other faceting minor phases grow as fibres but following most tortuous paths, the Zn-rich fibres of the Sn–Zn eutectic tend to be easily resolved in an optical microscope and can be seen to lie generally along the growth axis of the specimen (Figs. 5c, d).

The reason(s) for the absence of dendrites and the near axial fibres of the Sn–Zn eutectic are unclear. However, this behaviour is not confined solely to the Sn–Zn eutectic since similar microstructures may be observed for the Bi–Ag eutectic. Both systems display very stable lattice parallelism and habits to the extent that the usual "fanning-

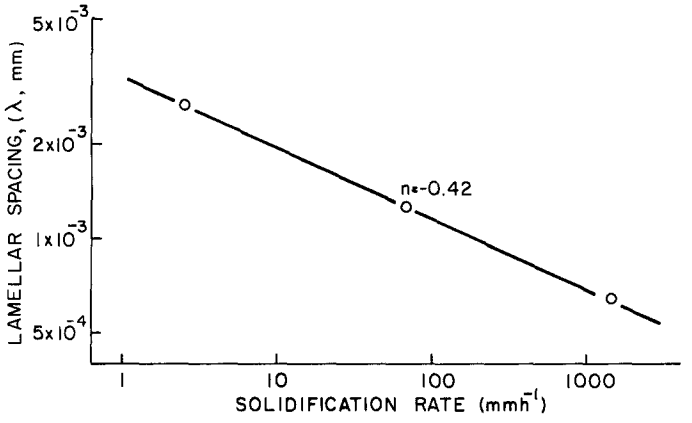

Figure 6 Effect of solidification rate (R) on the lamellar spacing (λ) of directionally solidified Sn–Zn eutectic alloys.

out" characteristic of colony formation during cellular growth is absent until marked constitutional supercooling arises [23].

The entropy of solution (ΔS) of the Zn-rich phase in the Sn–Zn eutectic is 7.6 cal $K^{-1}mol^{-1}$ and that of Ag in the Bi–Ag eutectic is 9.0 cal $K^{-1}mol^{-1}$ [1]. Since faceting tends to occur if $\Delta S > 5.5$ cal $K^{-1}mol^{-1}$, then both Ag and Sn would tend to facet strongly and so a pronounced growth rate anisotropy might be expected to result. During rapid growth, this should lead to repeated overgrowth by the matrix and so the fibres would be caused to follow a tortuous path, as is generally the case [5].

Unfortunately, entropy of solution data is not available for the Cd–Ge system but the Ge phase behaves much like that of Si in the Al–Si eutectic.

Elliott and Moore [24] found that the more fibrous form of the Sn–Zn eutectic grows with only approximately 1° C when $R = 600$ mm h^{-1} whereas the fibrous form of silicon ("modified") in Al–Si grows with an undercooling of 12 to 14° C [25]. Most other systems involving a covalently bonded minor phase also display marked undercooling when freezing as the modified eutectic [26]. In view of this, and noting the marked similarity of the Sn–Zn and Bi–Ag systems, it is presumed that the absence of primaries and the presence of near axial fibres of the minor phase in these systems when frozen rapidly is due to the fact that both minor phases have metallic bonding and can be caused to grow rapidly in a coupled manner at only small undercooling.

4.2. Mechanical properties

The increase in strength with increasing growth rate is a common feature of the mechanical properties of most unidirectionally grown eutectics. It is usually associated with the manner in which structural refinement leads to increased dislocation pile-up during deformation [27]. The plateau observed in both the tensile and compressive strengths for $R > 1000$ mm h^{-1} should be contrasted with the decrease in strength at high growth rates observed in the Pb–Cd [8] and Sb–Ge systems [9] and the continuous rise in Cd–Zn [7]. The decrease was associated with the marked lamellar misalignment and irregularity resulting from cellular growth in the Pb–Cd eutectic and with the presence of brittle Sb-rich dendrites in the Sb–Ge eutectic. With Cd–Zn although cellular growth occurred at very high growth rates, the misalignment tended to be small. In the case of Sn–Zn, the specimens contained no dendrites at any of the growth rates used and since relatively less misalignment occurred as compared with Pb–Cd, little or no "falling-off" of strength with increasing rate of growth might be expected.

It is of interest to attempt a rule of mixtures calculation for the Sn–Zn eutectic composite, namely

$$E_c = E_f V + E_m V_m \qquad (2)$$

where V is the volume fraction and the subscripts c, f and m refer to composite, fibre and matrix, respectively. Since the minor phase lamellae are well-separated in a broken-lamellar eutectic, little "matrix constraint" might be expected [9].

It was found that Young's Modulus (E) for the specimen grown at 12 mm h^{-1} was 60.9×10^3 Nmm^{-2} (8.9×10^6 psi) and for that grown at 120 mm h^{-1} it was 69.1×10^3 Nmm^{-2} (10.1×10^6 psi). Using the upper value and assum-

TABLE 1 Mechanical properties of directionally solidified Sn–Zn eutectic alloys (at 25° C).

Growth rate ($mm\ h^{-1}$)	Microstructure	Tension				Compression				
		0.2% off-set yield strength ($N\ mm^{-2}$)	UTS ($N\ mm^{-2}$)	Uniform elongation (%)	Work hardening index (n)	0.2% off-set yield strength ($N\ mm^{-2}$)		UCS ($N\ mm^{-2}$)		Uniform contraction (%)
						As-grown	Quenched*	As-grown	Quenched*	
5.1	Broken-lamellar	33.0	49.4	1.0	0.13	62.3	79.4	64.2	95.6	1.3
12.0	Broken-lamellar	–	54.7	–	–	58.5	80.8	65.6	89.9	2.2
53.0	Broken-lamellar	40.3	52.8	1.3	0.25	68.0	90.8	82.3	101.3	1.6
120.0	Broken-lamellar	45.8	70.4, 71.8	2.1	0.29	76.1	85.6	91.8	97.9	1.7
420.0	Broken-lamellar	59.0	81.8	1.4	–	99.8	88.9	111.7	99.8	0.9
780.0	Broken-lamellar/Fibrous	65.1	78.4	1.6	0.25	101.7	75.1	117.9	85.6	1.8
1105.0	Broken-lamellar/Fibrous	71.8	95.0	2.3	0.24	98.9	61.3	130.7	73.2	1.8
2800.0	Broken-lamellar/Fibrous	70.4	80.8, 77.5	1.5	–	111.7	59.0	127.4	77.5	1.3
4000.0	Fibrous	69.4	89.9	1.1	0.24	116.5	62.3	133.6	78.4	2.0
As cast	Fibrous	–	–	–	–	24.5	–	54.7	–	–

*The "as-grown" samples were maintained at 190° C for 5 min and then water-quenched.

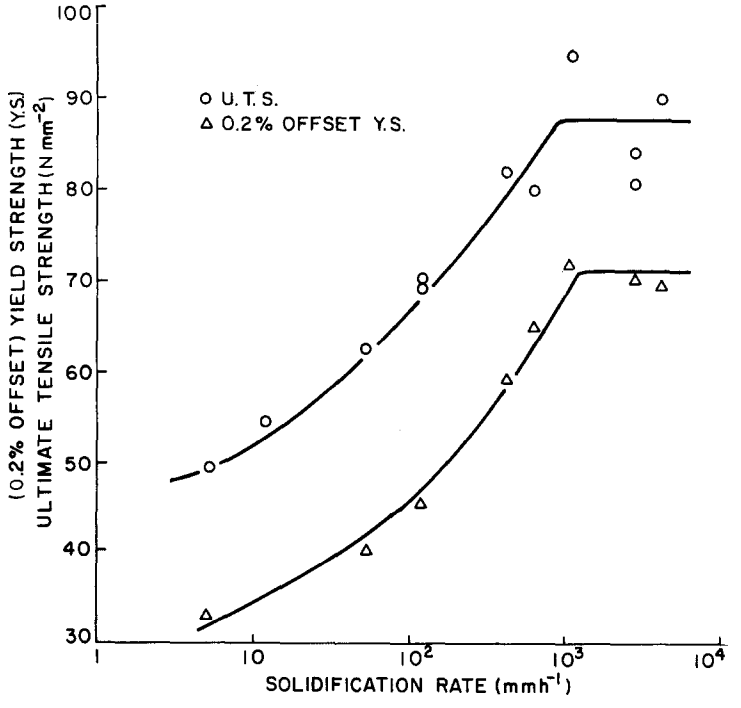

Figure 7 Effect of solidification rate on the yield strength (0.2% off-set) and ultimate tensile strengths of the directionally solidified Sn–Zn eutectic composite.

ing the rule of mixtures holds, with a volume fraction of zinc of 8.3% and $E_{\langle 11\bar{2}0\rangle} = 119 \times 10^3\,\mathrm{Nmm^{-2}}$ (17.2×10^6 psi) for zinc [28], we may calculate E for the Sn-rich matrix, namely, $65.0 \times 10^3\,\mathrm{Nmm^{-2}}$ (9.5×10^6 psi). This may be compared with the published values for E_{Sn} [29]. They are $E_{[001]} = 84.2 \times 10^3\,\mathrm{Nmm^{-2}}$ (12.3×10^6 psi), $E_{[110]} = 26.0 \times 10^3\,\mathrm{Nmm^{-2}}$ (3.8×10^6 psi) and $E_{\text{Fine-grained polycrystal}} = 44.5 \times 10^3\,\mathrm{Nmm^{-2}}$ (6.5×10^6 psi). The orientation relationships for the Sn–Zn eutectic have been reported as [30].

$$(100)_{Sn} \parallel (0001)_{Zn}$$

$$[001]_{Sn} \parallel [01\bar{1}0]_{Zn}$$

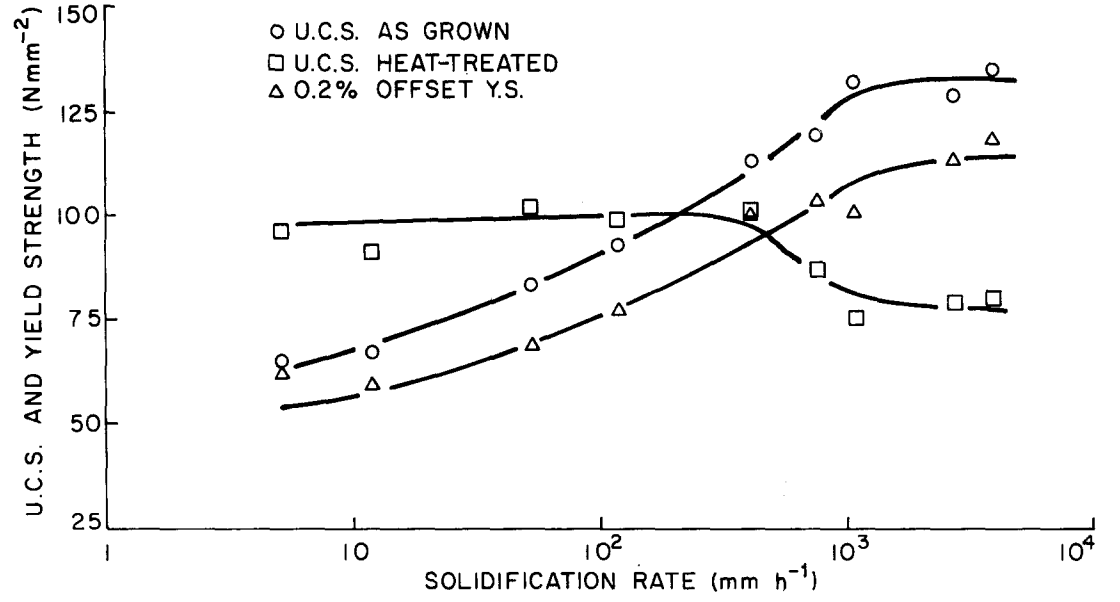

Figure 8 Effect of solidification rate on the yield strength (0.2% off-set) and ultimate compressive strengths of the directionally solidified Sn–Zn eutectic composite in the "as-grown" and heat-treated condition.

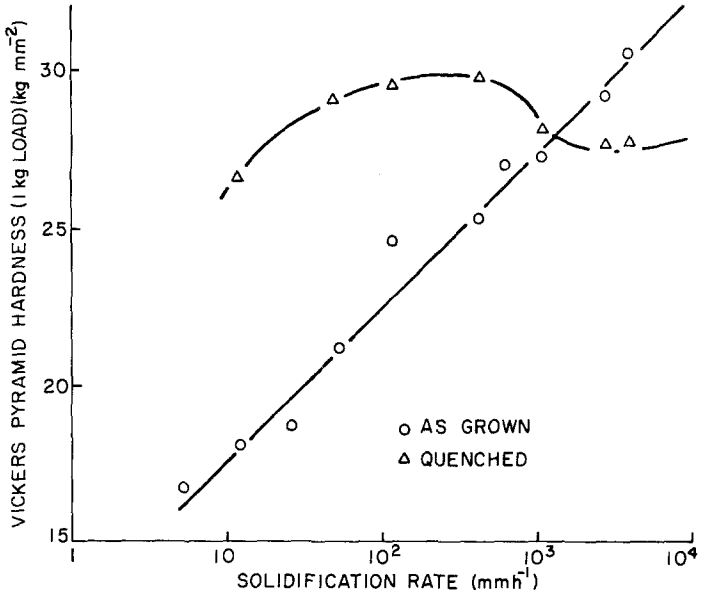

Figure 9 Effect of solidification rate on the hardness of the directionally solidified Sn–Zn eutectic composite, in the "as-grown" and heat-treated condition.

with a habit $(101)_{Sn} \| (10\bar{1}2)_{Zn}$ and a growth direction $[120]_{Sn} \| [01\bar{1}0]_{Zn}$. Since the growth direction lies in the $(001)_{Sn}$ and within 15° C of the $[110]_{Sn}$ in which Young's Modulus is $26.0 \times 10^3 \text{Nmm}^{-2}$, it has been presumed that $E_{[120]}$ is of the order of 30 to $40 \times 10^3 \text{Nmm}^{-2}$. When this is compared with the calculated value of $65 \times 10^3 \text{Nmm}^{-2}$ for the matrix on the basis that the rule of mixtures might apply, it must be concluded that matrix constraints are significant.

In doing this calculation, it may be inappropriate to use the only published bulk value for E_{Zn}, namely that for the $[11\bar{2}0]$ direction since the Zn-rich phase grows with $[01\bar{1}0]$ direction. Mechanical testing of Zn whiskers of diameter 1 to 10 μm whose axes lay in the $(10\bar{1}0)$ plane gave experimental values consistently smaller, namely 0.7 x (bulk value) [31]. This difference has usually been ascribed to surface flaws in the whiskers. However, since the thickness of the Zn-rich phase in the Sn–Zn eutectic is comparable with that of the whiskers, and there is no reason to suppose that the surfaces of the lamellae do not possess stress raisers, it may be more appropriate to use a value of 0.7 $(119 \times 10^3) = 83.3 \times 10^3 \text{Nmm}^{-2}$ for E_{Zn}. Using this, the presumed Young's modulus of the Sn-rich matrix becomes slightly higher, namely, $67.8 \times 10^3 \text{Nmm}^{-2}$ $(9.9 \times 10^6 \text{ psi})$, implying even greater matrix constraints.

The changes in hardness with growth rate are all the more interesting since the curve of VPN versus R does not fall off at higher growth rates

TABLE II Hardness of Sn–Zn eutectic alloys in as-grown and quenched condition as measured on transverse sections perpendicular to the growth direction

R (mm h^{-1})	VPH (load 1 kg) (kg mm^{-2})		UTS*	UCS*
	As-grown	Quenched	VPH	VPN (as-grown)
5.1	16.8		0.30	0.39
12.0	18.1	26.6	0.30	0.37
26.0	18.7			0.40
53.0	21.2	29.0	0.30	0.40
120.0	24.6	29.5	0.29	0.38
420.0	25.3	29.7	0.33	0.45
780.0	27.0		0.30	0.46
1105.0	27.2	28.1	0.36	0.49
2800.0	29.2	27.6	0.29	0.45
4000.0	31.5	27.7	0.29	0.43
As cast	20.2	24.5		

*kg mm^{-2}.

TABLE III Effect of annealing on the mechanical properties of unidirectionally-grown Cd–Zn eutectic alloys.

Growth Rate ($mm\,h^{-1}$)	Microstructure	Compression			
		0.2% off-set Y.S. ($N\,mm^{-2}$)		UCS ($N\,mm^{-2}$)	
		As-grown	Quenched*	As-grown	Quenched*
4.0	Regular lamellar	193	307	211	324
400.0	Regular lamellar	326	406	329	421
4000.0	Fibrous	321	303	427	362

*The as-grown samples were maintained at 250° C ($0.95T_m$) for 5 min and then water-quenched.

as do the UTS versus R and UCS versus R plots. The reason for this is unclear but may be associated with the fact that the strain field around the hardness indention is roughly hemispherical and so is only likely to be sensitive to the state of refinement of the Zn-rich phase rather than its degree of axial alignment.

A relation between the Vickers hardness number and the ultimate tensile strength has been derived by Tabor [32] according to which

$$\frac{\text{UTS}}{H} = \frac{(1-n)}{2.9}\left|\frac{12.5n}{1-n}\right|^n \qquad (3)$$

where n = work-hardening index.

J. R. Cahoon [33] simplified this expression to

$$\frac{\text{UTS}}{H} = 0.345\left|\frac{n}{0.217}\right|^n \qquad (4)$$

The ratios of UTS/H and UCS/H are tabulated in Table II.

It is interesting to note that for $R \leqslant 120\ mm\,h^{-1}$, the UTS/$H$ and UCS/H ratios are almost constant, though not equal.

The values of work hardening exponents were determined graphically from the plots of log σ versus log ϵ (where σ and ϵ are engineering stress and strain respectively) and are listed in Table I. The comparison between the observed and calculated UTS/H ratios is given in Table IV. It is interesting to see such a relatively good fit since an earlier detailed study [34] of the correlation of changes in hardness and of tensile and compressive properties with the rate at which Al–Si eutectic alloys were frozen gave only a weak correlation of VPN and UCS.

Returning to the effect of quenching on the Sn–Zn specimens, from other studies [19] we would expect quenching to increase the hardness of the more slowly grown samples. However, the reduced values of the more rapidly grown samples were unexpected. We must presume that the time spent at the annealing temperature was sufficient for some structural degeneration to occur in the more fibrous specimens although none was apparent from optical examination. Our studies of the thermal stability of the Cd–Zn eutectic [34] and Pb–Cd eutectic [35] shows that a 5 min anneal at approximately 0.95 of the eutectic melting temperature can bring about significant but subtle changes in the microstructure and so produce a reduction in strength. This then is the reason for the decrease in strength of the heat-treated, more rapidly grown Cd–Zn specimen.

The increased strength induced by quenching the Cd–Zn specimens grown slowly is probably solution strengthening since fast diffusion is not known in this system. However, the solubility limit of Cd in Zn and Zn in Cd at the eutectic temperature (266° C) are 2.15 and 2.95 wt% respectively. Since the solubilities at 100° C approach zero, rapid quenching would give some supersaturation and induce solute hardening. The deformation mode appeared to be solely by slip in the Sn-rich matrix and that in the Zn-rich phase to be unresolvable due to the fineness of the structure.

In view of the fact that behaviour similar to

TABLE IV Comparison of the observed and calculated values of UTS/H [33]

Growth Rate ($mm\,h^{-1}$)	n	UTS/H (observed) ($kg\,mm^{-2}$)	UTS/H (calculated from Equation 4) ($kg\,mm^{-2}$)
5.1	0.13	0.30	0.32
53.0	0.25	0.30	0.36
120.0	0.29	0.29	0.37
780.0	0.25	0.30	0.36
1105.0	0.24	0.36	0.35

that found in Sn–Zn is observed in Cd–Zn, and other systems [36], the strengthening induced in the slowly grown Sn–Zn eutectic alloys cannot be unequivocally ascribed to the trapping of Zn in semi-interstial sites in the Sn-rich matrix.

5. Conclusions

(1) The Sn–Zn eutectic has been directionally solidified at rates from 5 to 4000 mm h^{-1}. The structure is primarily broken-lamellar but becomes fibrous for growth rates exceeding 1000 mmh^{-1} the fibres tending to remain axial. Occasional grains are fibrous at lower growth rates. No dendrites of the major phase were seen at any growth rate.

(2) Room temperature tensile and compressive strengths were found to increase with growth rates up to $R = 750$ mm h^{-1} above which they assumed steady values. This is attributed to some loss of fibre alignment at higher growth rates. The deformation mode was slip.

(3) Room temperature hardness values were found to increase monotonically with growth rates up to 4000 mm h^{-1}, the largest growth rate used. This is considered to be due to the omni-directional nature of the strain field surrounding the indentation resulting in a hardness dependence which depends only on structural refinement.

(4) Annealing at near-eutectic temperatures of Sn–Zn and, for comparison, Cd–Zn eutectic alloys followed by quenching results in similar results for both systems, namely, increased strength for $R < 750$ mm h^{-1} and decreased strength above. The former is considered to be due to solution hardening and the latter to structural degradation at the annealing temperature. These experiments were unable to resolve whether the fast diffusion nature of Zn in Sn was of significant influence.

Acknowledgements

The authors wish to acknowledge the financial support of the National Research Council of Canada and of Queen's University.

References

1. M. N. CROCKER, R. S. FIDLER and R. W. SMITH, *Proc. Roy. Soc.* **A335** (1973) 15.
2. M. N. CROCKER, M. MCPARLAN, D. BARAGAR and R. W. SMITH, *J. Crystal Growth* **29** (1975) 85.
3. M. N. CROCKER, D. BARAGAR and R. W. SMITH, *ibid.* **30** (1975) 198.
4. M. SAHOO and R. W. SMITH, *Metal Science* **9** 1975) 217.
5. *Idem, Can. Met. Quart.* **15** (1976) 1.
6. *Idem, J. Mater. Sci.* **11** (1976) 1125.
7. *Idem, ibid.* **11** (1976) 1680.
8. *Idem, ibid.* **13** (1978) 283.
9. *Idem, ibid.* **13** (1978) 1565.
10. M. SAHOO, G. W. DELAMORE and R. W. SMITH, *ibid.* **15** (1980) 1097.
11. R. P. ELLIOT, "Constitution of Binary Alloys", First Supplement, (McGraw Hill Inc., New York, 1965).
12. P. J. TAYLOR, H. W. KERR and W. C. WINEGARD, *Can. Met. Quart.* **3** (1964) 235.
13. H. W. KERR and W. C. WINEGARD, *Can. Met. Quart.* **6** (1967) 67.
14. R. W. FIDLER, J. A. SPITTLE, M. R. TAYLOR and R. W. SMITH, Publication 110 (The Solidification of Metals, Iron and Steel Inst., London, 1968) p. 173.
15. D. JAFFREY and G. A. CHADWICK, *Trans. Met. Soc. of AIME* **245** (1969) 2435.
16. G. A. CHADWICK, *J. of Metals* **92** (1963-4) 18.
17. W. A. TILLER, "Liquid Metals and Solidification" (American Society for Metals, Metals Park, Ohio, 1958) p. 276.
18. W. A. TILLER and R. MRDJENOVICH, *J. Appl. Phys.* **34** (1963) 3639.
19. F. VNUK, M. Sc. Thesis, University of Birmingham, 1968.
20. B. F. DYSON, *J. App. Phys.* **37** (1966) 2375.
21. F. H. HUANG and H. B. HUNTINGDON, *Phys. Rev. B.* **9** (1974) 1479.
22. F. VNUK, M. H. AINSLEY and R. W. SMITH, unpublished work.
23. R. S. FIDLER, Ph.D. Thesis, Birmingham University, 1969.
24. R. ELLIOT and A. MOORE, *Scripta Met.* **3** (1969) 249.
25. R. W. SMITH, "The Solidification of Metals" *Iron and Steel Inst. Special Report, London,* **110** (1968) 226.
26. D. BARAGAR, M. SAHOO, and R. W. SMITH, "Solidification of Metals and Castings" (The Metals Society, London, 1979) p. 88.
27. H. BIBRING, Proceedings of the Conference on *In-Situ* Composites, Vol. II (National Academy of Eng., Washington, D.C., 1973), P. 1.
28. H. B. HUNTINGDON, *Solid State Phys.* **I** (1958) 278.
29. "Properties of Tin" (Tin Research Institute, Middlesex, England, 1954) p. 42.
30. "Advances in Materials Research", edited by Herbert Herman, Vol. 5 (Willey-Interscience, New York, 1971), p. 134.
31. R. V. COLEMAN, B. PRICE and N. CABREVA, *J. App. Phys* **28** (1957) 1360.
32. D. TABOR, "The Hardness of Metals" (Oxford University Press, Oxford, 1951) p. 107.
33. J. R. CAHOON, *Met. Transactions* **3** (1972) p. 3040.
34. R. VAN DER MERWE, M. SAHOO, R. W. SMITH, Conference on *In-Situ* Composites–III (Ginn Custom Publishing, Lexington, 1979) 107.
35. *Idem,* Ph.D. Thesis, Queen's University, 1980.
36. R. W. SMITH, unpublished work.

Received 8 February and accepted 20 March 1980.